

THE INSTITUTE FOR ANALYTICAL PHILATELY, INC.

Proceedings of the Fifth International Symposium on Analytical Methods in Philately

10 & 17 October 2023

Edited by

Thomas Lera, John H. Barwis, and Kenneth R. Nilsestuen



Abstract

Lera, T., Barwis, J. H., and Nilsestuen, K. R. *Proceedings of the Fifth International Symposium for Analytical Methods in Philately*. x + 120 pages, 95 figures, 16 tables, 2023. This publication contains papers presented at the Fifth International Symposium on Analytical Methods in Philately, hosted by Institute for Analytical Philately, Akron, OH., on October 10 and 17, 2023. The eleven papers describe a wide range of techniques for stamp identification and expertizing. Several describe the use of visible, infrared, and ultraviolet light to discriminate among printings of the same design. Others report nondestructive analyses of ink chemistry to document how inks were modified over time. Together the papers illustrate philatelic applications of a wide range of equipment, including desk-top scanners, Video Spectral Comparator (VSC), X-Ray Fluorescence (XRF), Scanning Electron Microscope (SEM), X-Ray Diffraction (XRD), Fourier-Transform Infrared Fluorescence (FTIR), Energy Dispersive X-Ray Reflectance Spectrometer (EDS), Attenuated Total Reflectance Spectroscopy (ATR), and ultraviolet fluorescence.

Published by The Institute for Analytical Philately, Inc.

6685 Cuttalossa Road
New Hope, PA 18938

© 2023 by The Institute for Analytical Philately.

Design and Layout: Kenneth Trettin

Printed: Wilcox Printing & Publishing, Inc., 102 S. Main St., Madrid, IA 50156, U.S.A.

Compilation copyright © 2023 The Institute for Analytical Philately, Inc.

The Scott Numbers are the copyrighted property of Amos Media Company and are used here under a licensing agreement with Amos. The marks SCOTT and SCOTT'S are Registered in the U.S. Patent and Trademark Office, and are trademarks of Amos Press, Inc. dba Scott Publishing Co. No use may be made of these marks or of material in this publication which is reprinted from a copyrighted publication of Amos Press, Inc., without the express written permission of Amos Media Co., Sidney, OH 45373.

The rights to the text and images in this publication, including cover and interior design, are owned by The Institute for Analytical Philately, Inc. contributing authors, or third parties. Use of materials is permitted only for personal, educational, or noncommercial purposes. Users must cite author and source of content, must not alter or modify copyrighted content, and must comply with all other terms or restrictions that may be applicable. Users are responsible for securing permission from a rights holder for any other use.

Regarding illustrations: The illustrations in this book have been sized to fit the constraints of the page size and the editor's layouts. Illustrations may be reduced or enlarged as necessary without any attempt at keeping all illustrations to scale.

ISBN: 979-8-218-19789-6

Library of Congress Control Number: 2023907981

Color Analysis and Microfade Testing of the 1918 Curtiss Jenny U.S. Airmail Stamp

Thomas Lam¹, Susan Smith², Scott Devine², and Edward P. Vicenzi¹

Abstract

The Inverted Jenny is the best recognized stamp in the United States and is displayed in the National Postal Museum's *Gems of American Philately* exhibition. A careful approach to exhibition management, including a conservative lighting plan, has allowed the museum to permanently exhibit some of its most precious objects such as the Jenny without subjecting the objects to unnecessary light exposure. One goal of this study is to determine if the museum's current exhibition practices are effective in protecting such rare philatelic objects given we know very little about the Jenny's blue and red inks or how they interact with exposure to light.

Since the Inverted Jenny could not be used for testing, surrogate stamps were purchased and their colors analyzed and verified using color reference materials designed specifically to resist fading. Two independent systems were used for the color measurements and were found to be comparable despite differences in the instrumentation. One of the replicate stamps was subjected to accelerated light exposure under controlled conditions and its colors measured at the end of the testing period to simulate the impact of long-term exhibition lighting.

The measurements demonstrated that there is not a single-color value that represents the red, blue, and uncolored regions even within a single Jenny. These regions faded, or experienced shifts in color, at different rates with exposure to light; the stamp paper changed at the same rate as the blue regions, with the red regions shifting in color at a slower pace. These color shifts act upon the spread of red, blue, and paper colors measured before accelerated laboratory tests were performed, highlighting the importance of the understanding the initial range of color

variability, as well as the need to consider the impact of exhibit lighting versus daylight/sunlight on stamp coloration. Ultimately, both the stamp paper and the colors of the Jenny were determined to be stable with respect to the lighting plan developed for the Inverted Jenny at the National Postal Museum.

Introduction

Less than fifteen years after the Wright brothers' first successful sustained flight by a piloted aircraft, the US Post Office Department offered special delivery airmail service and the Bureau of Engraving and Printing (BEP) issued a striking red and blue 24¢ Curtiss Jenny postage stamp. The stamp is commonly referred to as "the Jenny" after the US Army's Curtiss aircraft that carried mail on the inaugural flights in May 1918. The stamp is not only recognized as the first US airmail stamp, but also the first stamp issued worldwide for regular airmail service and the first bi-colored airmail stamp (Kirker 2006). The Jenny is best known for the single sheet of 100 stamps in which the plane was printed upside down. As a result of this printing error, the inverted Jenny is the best recognized stamp in the United States.

Despite the stamp's popularity and although much is known about its design and printing, we are unaware of information regarding the material

¹Smithsonian Institution, Museum Conservation Institute, Suitland, MD 20746

²Smithsonian Institution, National Postal Museum, Washington, D.C. 20002

properties of the inks used and their susceptibility to light exposure. It has been known for some time that the BEP's Engraving Division's Stamp History for the 24¢ Air Mail Stamps (Airplane), Series 1918, contains a level of uncertainty regarding ink formulation and nomenclature within the records (Engraving Division 1960). Given the short period of time during which the stamps were printed, roughly two months, it is reasonable to assume however that the ink formulations and materials did not change during production.

The period during which the Jenny was produced was a difficult one at the BEP, as it was in the US as a whole. World War I created challenges for the BEP, including its inability to take delivery of Prussian Blue and red (referred to as "standard red" or "printing red S225" in documents) dry color or powder pigments from Germany (Gebr. Heyl & Co. 1917, Treasury Dept. to Speaker of the House 1917) and difficulties "obtaining steel of the proper degree of hardness" (N. Underwood to James Wilmeth 1918) to replace worn printing plates. The war also necessitated staffing shifts to print "the more important [war] bonds" (James Wilmeth to Wilfred A. French 1918). There was also the lack of sufficient machinery to handle the printing needs, leading to the use of a retired hand-roll printing press (the spider press) to print this air mail special delivery stamp. With all the ongoing issues during that period, it is surprising that the decision was made to create a bi-color intaglio stamp, which was a labor and supply intensive process. The turn around time from the creation of the dies from May 4 – 10 to the printing of plate proofs on May 10 and 11, to the delivery of the first stamps to the main Washington DC post office on May 13 represented an accelerated production schedule (Engraving Division 1960). The patriotic color selection for the Jenny together with the stamp's novel purpose and the high cost at 24¢ was eight times the general cost of a 3¢ (USPS 2022); underscore the importance of the project of America's first postage stamp for airmail.

The research and exhibition value of historic stamps is often dependent upon the condition of the paper substrate and subtle nuances of color in the printing inks and dyes, so extended or recurring exhibitions of rare and unique objects like the Inverted Jenny present a challenge. Exposure to light causes irreversible damage to some materials. Visible light damage may include aesthetic changes such as fading or color shifts, while prolonged exposure may lead to structural damage including embrittlement

of paper-based objects. Current museum lighting standards were developed in the 1970s with a focus on reducing visible light to only what is needed to sufficiently view the object, and eliminating ultraviolet light altogether when exhibiting light sensitive objects such as paper and textiles (Thomson 1978).

The National Postal Museum (NPM) limits exposure of paper-based objects to 54 Candela steradian/square meter (the equivalent of 5 footcandles (fc) or 54 lux) for no more than three to six months at a time assuming eight to ten hours of exhibition per day. To exhibit rare philatelic materials for longer periods, NPM employs various strategies including wall mounted pullout frames, motion sensors, and SmartGlass technology, all of which ensure that objects are illuminated only when being viewed by a visitor. These specific technologies, combined with custom-designed exhibit spaces and a program of ongoing monitoring, allow for the creation of customized lighting plans for a range of philatelic and postal history objects.

Balancing light exposure with the need to make objects available for short term display as well as long term exhibition is a complex formula that relies on understanding the material composition of the object, the nature of the light source, and careful management of the light level. The research discussed here addresses the fading properties of postage stamps by using a set of color-based spectrometry tools to quantitatively measure colors and evaluate the nature of the color change imposed by exposure to museum lighting. One of the goals of this study is to determine if that the already conservative approach being taken at the National Postal Museum is not significantly damaging collection material. A second goal is to show that the current exhibition practices are effective in preserving these objects for future generations, in part by estimating long term cumulative illumination exposure.

Materials and Methods

Materials

The 24¢ Curtiss Jenny postage stamp was chosen for this study for reasons related to the stamp's bi-colored design, the availability of surrogate copies for testing, and the notoriety of the famous "inverted Jenny." In this study, research was performed on six Jenny stamps (Figure 1A) with a seventh stamp on cover (Figures 1B and C). Similar to other philatelic studies, information from plate proofs can strengthen philatelic research (DeBlois and Harris 2011, Charles



Figure 1. Curtiss Jenny stamps and additional materials used in this study. A) Images of the six objects examined, each stamp is 2.0 cm x 2.5 cm (with the red frame being 1.9 cm x 2.2 cm) B) An enlarged view of the Jenny on cover with regions of interest for the substrate paper, blue, and red regions highlighted in black-, cyan-, and white-unfilled circles. C) Image of Jenny 7 cover and the vendor-supplied white reference tile. D) Blue vignette for 24¢ stamp; plate number 8493 (National Postal Museum, Object number 0.242263.15824) printed on paper of height x width: 27.94 x 46.04 cm (11 x 18 1/8 in.). E) 24¢ carmine frame for USA Scott C3; plate number 8492 (National Postal Museum, Object number 0.242263.15825) printed on paper of height x width: 28.58 x 35.56 cm (11 1/4 x 14 in.).

2017, Charles 2020). The blue and red plate proofs from BEP plates 8493 (Figure 1D) and 8492 (Figure 1E) were made available for analysis from the Smithsonian's National Postal Museum (NPM). These proofs are from the only two plates used for this 24¢ stamp. The proofs have experienced limited exposure to natural and artificial lighting given their continuous storage at the BEP and NPM for the last 100 plus years. Therefore, as trial impressions for a stamp that began production immediately following their printing, they likely represent the closest approximation to the original stamp colors available to researchers and the philatelic community.

Color measurement

The Foster and Freeman Video Spectral Comparator (VSC8000/HS) at the NPM was used to determine quantitative color. Six locations in each of the substrate paper, blue, and red regions were measured for each stamp as shown in Figure 1B. To obtain color information on the unpigmented region of the stamp a vendor-supplied white reference was used. For the red and blue color analysis, the paper substrate served as the white reference. Using the stamp paper as the white reference allows for the interpretation of the ink color in contrast to the surrounding substrate given that the substrate itself – the stamp paper – can influence/influences the color. In other words, measuring the color of the substrate enables the study to account for it. Forty-nine measurements from the north position of the red elliptical “24” region at the bottom right corner of stamp impressions in the red proof were obtained. While fifty measurements were collected from stamp impression in the blue proof. Additionally, 100 measurements in the top center unpigmented sky region were made on multiple regions of both proofs. For stamp 7 (Figure 1B and C), an additional series of eighteen data points were collected using the vendor provided white reference. Color analyses collected using the VSC represent point spectra obtained while viewing the stamp at a constant horizontal field width of ≈ 14.1 mm, and a circular region of interest for reflected light directed to the spectrometer was approximately 0.11 mm in diameter with a spectral resolution of 3 nm.

Experimental color fading

Microfade testing (MFT) was performed on Jenny 7. As the only Jenny stamp on a cover, its weighted surface kept it flatter and in a more stable position than individual stamps alone would have

been. This allowed for the same locations as the VSC color measurements depicted in Figure 1B to more easily be evaluated. MFT is a spectroscopy technique developed by Whitmore et al. (Whitmore, Pan et al. 1999) as a non-contact and “virtually non-destructive” method for determining small increments of reflectance color shift on cultural heritage materials (Ford and Druzik 2013). Using a xenon light source, this system generates a spectral distribution in the visible wavelength range from ≈ 370 nm to ≈ 760 nm (Whitmore, Pan et al. 1999), which has been filtered through parts from a “Fading Test System” (Newport Oriel Corporation). For MFT setup, a custom head serves multiple purposes as it: 1) enables the light source from a fiber optic cable held in the center of this mount to be readily focused on the target, 2) provides a fixed position for the spectrometer collection fiber that carries the detected signal is routed to the spectrometer at the one end, and 3) has a digital endoscope magnifier positioned at the opposite end that provides a microscale view of the target area (Figure 2A). Prior to collection of each series of color fading experiments, dark and white references were collected to mitigate potential drift of the reflected light signal. Manual insertion of a neutral density filter into the optical path reduced the light intensity and allowed for the safe navigation to regions of interest using the microscope image, and an example of the filtered spot is highlighted and shown in Figure 2B. With the neutral density filter removed, the illuminated spot is on the order > 1 mm (Figure 2C). Recent developments in the assessment of the light fading spot size indicate the full width at half the maximum (FWHM) to be < 1 mm (Świt, Gargano et al. 2021). Given the MFT measurement is dependent upon the working distance, a custom spacer ≈ 1.1 cm in height was additionally used to achieve a constant value, and this height above the target generated a focused spot for this optical geometry. With the focused spot on a region of interest, the visible reflectance signal sent to the spectrometer was recorded and stored using Spec32 acquisition software. Using a custom script (Laudato Beltran, Pesme et al. 2021), the International Commission on Illumination (CIELAB) color space coordinates L^* , a^* , b^* and color difference by ΔE_{ab}^* (also referred to as ΔE_{76}^*) were exported from the acquisition software for a near real time display (Robertson 1977). CIELAB color space coordinates of L^* is expressed on the z-axis and represents the lightness to darkness value, the a^* is for red/green axis, and b^* for the yellow/blue axis as shown in Figure 3A.

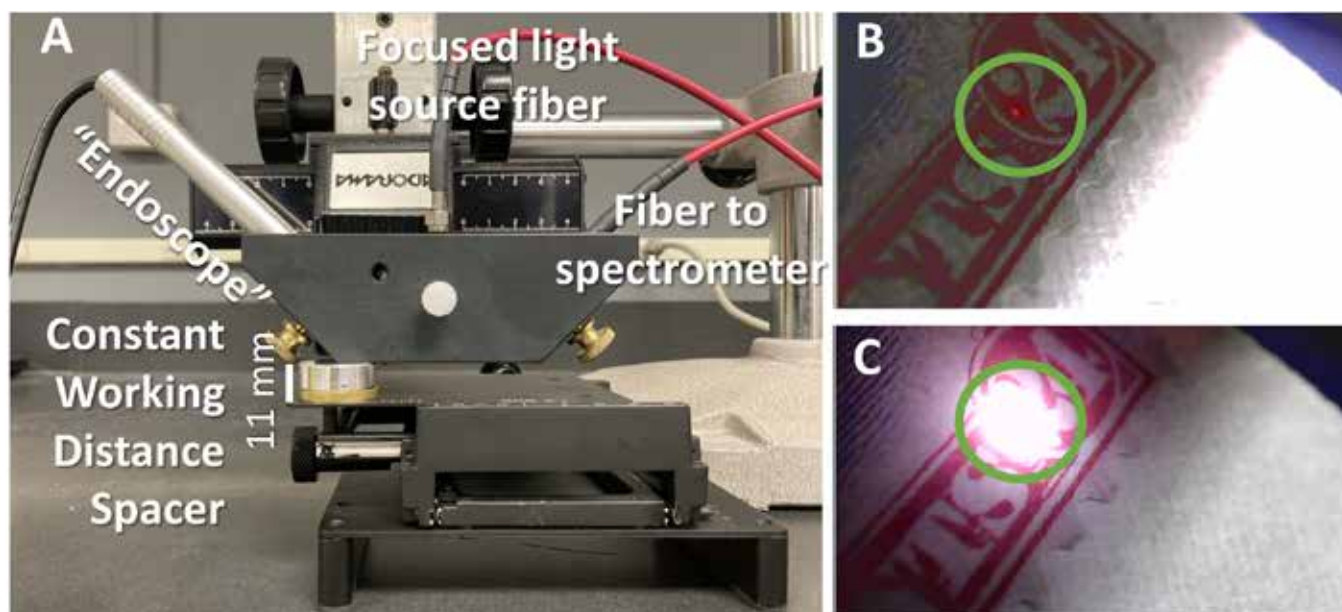


Figure 2. (A) Picture of custom mount used for Microfade testing. (B) Image obtained using the endoscope magnifier with the neutral density filter in place (C), and with the neutral density filter removed during data acquisition. Within this direction of the stamp in B and C there are 11 perforations along the 2 cm distance which is ≈ 0.18 cm per perforation.

Due to the challenges of accurately measuring the dose for a focused spot on the millimeter- to sub-millimeter-scale, coupled with run-to-run optical alignment variations of the MFT that are different from one MFT instrumental setup to another, a qualitative assessment of the relative kinetics of color fading was performed by comparing the stamp materials to different grades of International Organization for Standardization (ISO) blue wool standards that have documented light sensitivities (Materials Technology) (Lowe, Smith et al. 2017). In this study, ISO blue wool 1 and ISO blue wool 2 light fastness standards purchased from SDL Atlas USA (Rock Hill, SC) were used for the comparison. In the MFT data collection of the blue wool, the topography (height variation) of the weave is taken into consideration. Three measurements were collected for both blue wool 1 and blue wool 2. For each region of interest of the stamp to be evaluated, the test was performed for run durations of 300 seconds. (Materials Technology)

Color space

The CIE-L*a*b color model (Cibulski 2015, Judge 2015) and use of color difference by ΔE_{ab}^* (see glossary, equation 1) calculated from CIE-L*a*b are both color analysis expressions reported in the analytical philately literature (Hofmeyr 2020). For color analysis involving a single type of color and discussion regarding a specific color, the ΔE_{ab}^* color difference

method can be informational. Successful color analysis has also been demonstrated using other approaches, e.g. Red, Green, Blue (RGB) (Cibulski 2015, Cibulski 2015, Cibulski 2017); hue, saturation, and brightest (HSB) (Cibulski 2015, Mckee 2015, Hisey 2020); hue, saturation, and luminance (HSL) (Cibulski 2015, Cibulski 2017); CIE-L*(uv) plots (Allen and Lera 2012, Caswell 2012, Lera, Giaccai et al. 2012, Hofmeyr 2020), CIE-XYZ (Cibulski 2015), or analysis Romney Model in Munsell space (Judge 2015).

However, in quantitatively comparing the color difference among multiple colors, the color difference by ΔE_{ab}^* formula does not provide a complete analysis as it assumes that the CIELAB color space is perceptually uniform in the 3-dimensional (3D) color space, which it is not. The color difference by DE2000 or ΔE_{00}^* formula addresses this limitation. The color difference by ΔE_{00}^* takes into account the perceptual non-uniformities of the CIELAB color space by implementing five mathematical corrections to aspects of color attributes within the formula. (See glossary for details; Luo, Cui et al. 2001). Upon request, the authors can provide an Excel worksheet to convert color difference ΔE_{ab}^* values to the color difference ΔE_{00}^* values (Kuzio 2018). For this study, color difference by ΔE_{76}^* calculations have been applied to both VSC and MFT data. It should be noted that color difference by ΔE_{00}^* and color difference by

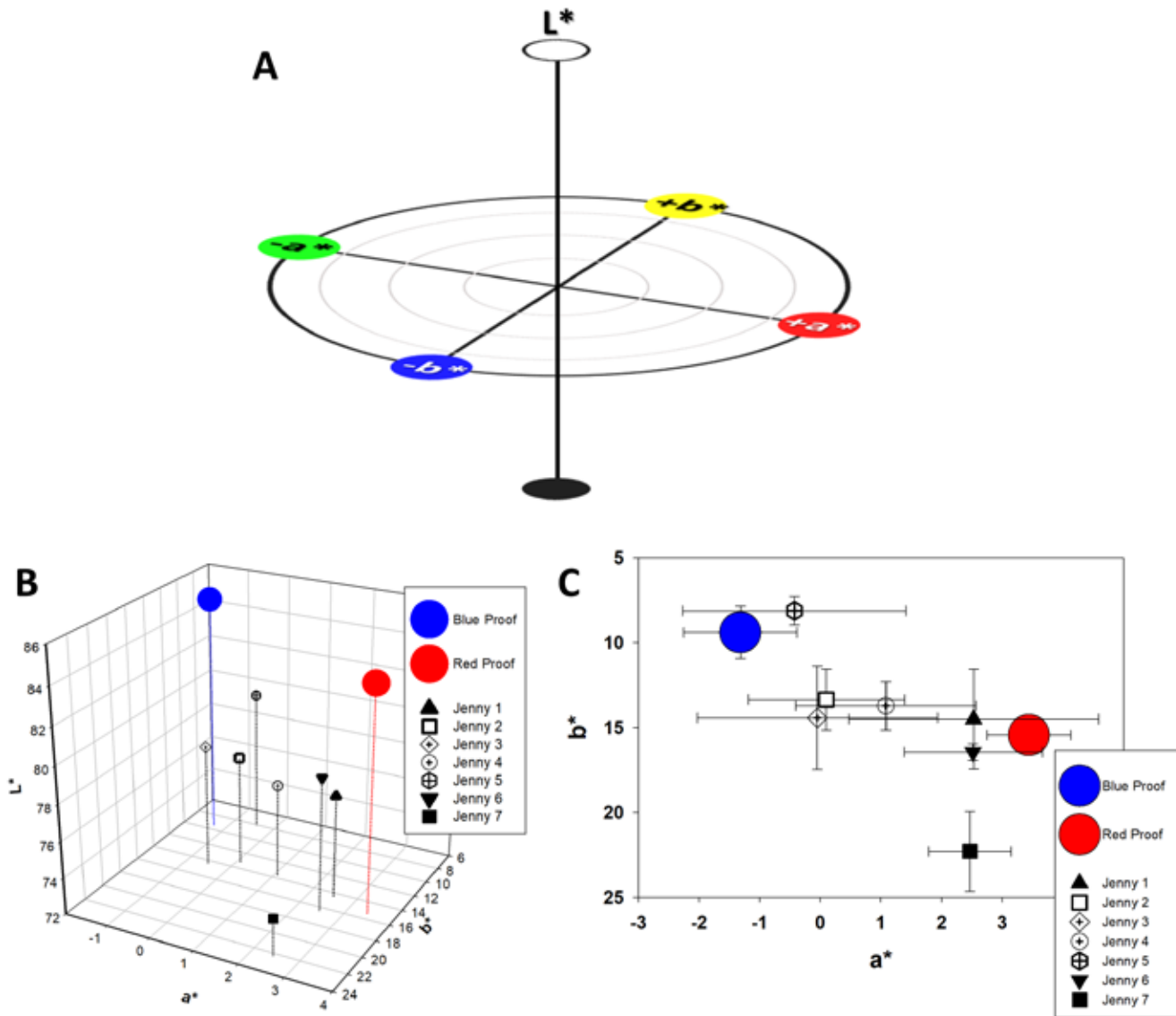


Figure 3. A) Schematic representation of color space showing end-member colors for a^* , b^* , and L^* intensities with concentric gray circles represent increasing chromaticity values outward from the origin. B) 3D plot of average values of L^* , a^* , and b^* for the paper substrates. C) 2D plot of the average values of a^* and b^* along with a^* and b^* uncertainties for the “white” data based upon population statistics.

ΔE_{ab}^* are not equivalent, and generally differ by a factor 2, where the color difference by ΔE_{ab}^* is typically the larger value (Ford and Druzik 2013).

To properly evaluate the accuracy of the color analysis carried out on the VSC and MFT, color measurements were also collected on red, green and blue light-fast ceramic tiles obtained from Hale Color Consultants, Inc., (Baltimore, MD) with reference tile colors traceable to the National Bureau of Standards (now the National Institute of Standards and Technology). Color visualization was performed using an online software tool to simulate the colors

seen by the spectrometers of the VSC and MFT by using the L^* , a^* , and b^* inputs. This software tool also converts color values between a variety of color models, including those found within philatelic literature e.g. RGB Adobe 98, HSLCIE- L^* ab , and CIE- $L^*(uv)$ (EasyRGB).

Statistical evaluation of color data

A variety of statistical approaches are available to determine which color measurements are equivalent to one another within uncertainty, or conversely, have differences that are significantly greater than expected by random chance. The statistical spread

of an average value of randomly distributed data is termed the standard deviation (σ) of the population. Since the deviation can be positive or negative, the spread of the data that results in plus or minus one or two standard deviations lies within the bounds of random chance to within 68 or 95 percent confidence respectively. In this study, the standard deviations reported represent the spread of the population of all color measurements and were calculated using an MS Excel 365 spreadsheet. The evaluation of the simple statistical output was made using analysis of variance (ANOVA), as well as through a comparison between each stamps' a^* and b^* color values to the Jenny blue and red proof "controls" using the Holm-Sidak method (see glossary) with a cutoff for dissimilarity at $> 95\%$ chance. The ANOVA computation was performed using Sigma Plot v14.5 (Inpixon) software.

Results

Color Analysis of the Stamp

Uncolored Paper

The uncolored regions of the Jenny are defined as areas free of any print mark or patterns and represent the stamp paper substrate. Figure 3B is a three-di-

mensional (3D) plot of the mean color values in terms of CIE L^* , a^* and b^* for measurements taken from the paper regions of the Jenny blue and red proofs, as well as for the paper locations described above for the seven Jenny stamps. (Figure 1B). L^* values of both the blue and red proofs are larger than those for the stamps. The differences in L^* were not unexpected since the proofs are on card (Robert A. Siegel Auction Galleries 2017) rather than on stamp paper. Figure 3C is two-dimensional (2D) plot of the mean values for a^* and b^* that yields a top-down projection of figure 3B with associated uncertainties to better describe the distribution of color values. Considering the spread of the mean values for the paper color of the seven stamps, Jenny 5 and Jenny 7 are $> 1 \sigma$ different in the b^* value, or the blue-yellow dimension (Figure 3A), relative to the cluster formed by the other five Jenny stamps.

As seen in Table 1, the simulated colors from the measured color values for the stamp papers do differ. In the examination of the paper regions the blue and red proofs (Figure 1D and 1E), the color difference is noticeable since we know they are not the same as the paper used in the stamp production. Given the proof papers were not used in production of the stamp, they do not represent a "control" for color analysis of the stamp paper, and therefore no color





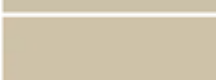




	L^*	a^*	b^*	Simulated Color
Blue Proof	85.05	-1.32	9.39	
σ	1.21	0.93	1.55	
Red Proof	84.17	3.44	15.44	
σ	0.92	0.69	1.16	
Jenny 1	77.65	2.53	14.50	
σ	0.74	2.06	2.95	
Jenny 2	78.07	0.10	13.35	
σ	1.11	1.29	1.81	
Jenny 3	78.72	-0.05	14.43	
σ	2.24	1.98	3.06	
Jenny 4	77.17	1.08	13.72	
σ	1.81	1.49	1.44	
Jenny 5	79.77	-0.43	8.12	
σ	1.04	1.84	0.84	
Jenny 6	79.27	2.52	16.45	
σ	1.57	1.14	0.49	
Jenny 7	74.03	2.47	22.30	
σ	0.68	0.68	2.35	

Table 1. Averages and standard deviations of the population for L^* , a^* , and b^* within the uncolored regions of the substrate paper for the proofs and stamps, along with their simulated color.

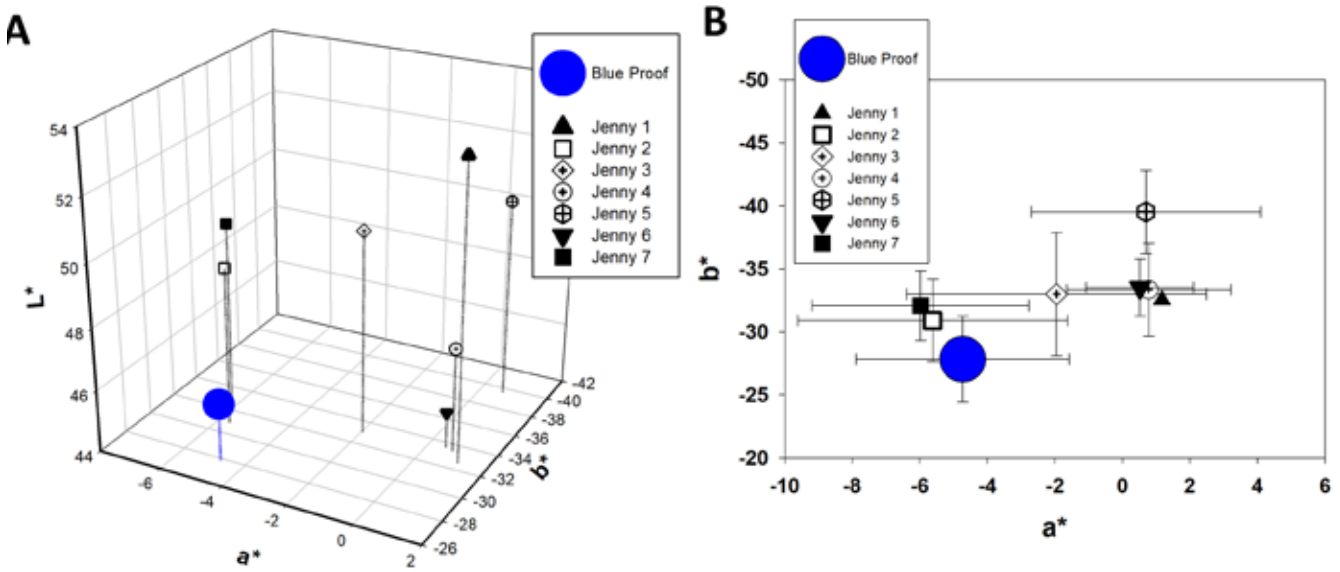


Figure 4. A) 3D plot of average values of L*, a*, and b* for the blue data B) 2D plot of the mean values of a* and b* with the a* and b* uncertainties represent the standard deviations of the population for the blue data.

difference by ΔE_{00}^* values were reported. The grayish blue simulated for the blue proof paper with a smaller b* value and the reddish tint in the red proof with a larger a* value are qualitatively consistent with the colors observed in the paper substrate in Figure 1D and 1E by naked-eye inspection. The color

simulation for Jenny 5 stands out as an outlier among the stamp papers, which is consistent with the visual observation that it was significantly “brighter” than the other six stamps and was indeed found to have the largest L* value.

Group Name	N (Sample Size)	Sample Mean	Standard Error of Mean	
			σ	$\sigma/(N^{0.5})$
Blue Proof	50	-4.73	3.16	0.447
Jenny 1	6	1.17	3.06	1.249
Jenny 2	6	-5.62	4	1.633
Jenny 3	6	-1.95	4.44	1.813
Jenny 4	6	0.78	2.44	0.996
Jenny 5	6	0.7	3.4	1.388
Jenny 6	6	0.52	1.59	0.649
Jenny 7	6	-5.98	3.21	1.31

Source of Variation	Degrees of Freedom (DF)	Sum of Squares (SS)	Mean Square (MS)	F	P
Between Groups	7	591.634	84.519	8.194	<0.001
Residual	84	866.409	10.314		
Total	91	1458.044			

Holm-Sidak:				
Comparison	Diff of Means	t	P	P<0.050
Blue Proof vs Jenny 1	5.9	4.252	<0.001	Yes
Blue Proof vs Jenny 4	5.51	3.971	<0.001	Yes
Blue Proof vs Jenny 5	5.43	3.913	<0.001	Yes
Blue Proof vs Jenny 6	5.25	3.784	0.001	Yes
Blue Proof vs Jenny 3	2.78	2.004	0.138	No
Blue Proof vs Jenny 7	1.25	0.901	0.603	No
Blue Proof vs Jenny 2	0.89	0.641	0.523	No

Table 2. ANOVA analysis for the blue colors with Holm-Sidak comparisons between the stamps and the blue proof control.

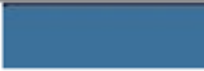







	L*	a*	b*	ΔE_{00}^*	Simulated Color
Blue Proof	45.87	-4.73	-27.82	NA	
σ	3.82	3.16	3.40	NA	
Jenny 1	53.45	1.17	-32.53	7.98	
σ	3.27	3.06	2.05	2.08	
Jenny 2	49.12	-5.62	-30.90	4.69	
σ	2.61	4.00	3.27	1.63	
Jenny 3	50.53	-1.95	-33.00	5.56	
σ	2.25	4.44	4.88	2.10	
Jenny 4	47.38	0.78	-33.35	4.84	
σ	4.13	2.44	3.70	1.92	
Jenny 5	50.43	0.70	-39.52	5.78	
σ	2.95	3.40	3.32	2.69	
Jenny 6	45.17	0.52	-33.53	3.86	
σ	3.02	1.59	2.25	1.73	
Jenny 7	50.15	-5.98	-32.08	5.04	
σ	2.97	3.21	2.76	3.18	

Table 3. Averages and standard deviations for L*, a*, b* measurements, and ΔE_{00}^* of the blue data for the proof and the Jenny stamps with their simulated color.

Blue Regions

The blue proof serves as a *de facto* color control based upon its controlled storage conditions with respect to light exposure. The average L* values of the blue proof were smaller than that for all the stamps, except Jenny 6 (Figure 4A). For the blue regions, Jenny 2, 3, and 7 are most similar to the blue proof both in terms of b* and a* data (Figure 4B). Figure 4B also shows that Jenny 5 is $> 1 \sigma$ different in the b* when compared to the blue proof. The analyses of variance of the blue data, along with comparisons of each stamp with the blue proof serving as a control, are shown in Table 2. Jenny 2, 3, and 7 were indeed determined to be statistically indistinguishable to the blue proof. In other words, the spread of blue color measured within Jenny 2, 3, and 7 falls within the range of blues measured in the proof to within a 95% confidence interval.

Though the graphical visualizations of the color data were useful, a table of values along with simulated colors demonstrates that Jenny 6 has the smallest calculated color difference by ΔE_{00}^* with a value of 3.86 and is qualitatively consistent with the simulated color for the blue proof. In this case, the ΔE_{00}^* calculation takes into account the smaller and more similar L* value of Jenny 6 in relation to the blue proof discussed above. Though Jenny 5 had the largest color difference in b*, it was not the stamp with the great-

est ΔE_{00}^* difference value in comparison to the proof. Jenny 1 had the greatest ΔE_{00}^* difference value, which also had the largest average L* value.

Red Regions

Applying the same methodology used for the blue proof above, the red proof can also be understood as a control for the red frame printed in 1918. In this case, the red proof has L* values intermediate to the distribution of means values for the Jenny stamps (Figure 5A). The top-down projection of figure 5A shows Jenny 7 was most similar to the red proof (Figure 5B). Jenny stamps 1, 2, 5, and 6 have statistical overlap with the red proof in the b*, or yellow-blue dimension. Conversely, relative to the red proof, Jenny 2-6 red data are $> 1 \sigma$ in the a*, or red-green dimension, with Jenny 4 exhibiting the greatest difference in a*. ANOVA results indicate Jenny 7 was most similar to the red proof among all stamps in both a* and b* dimensions (Table 4).

Consistent with Figure 5B, the tabulated values for ΔE_{00}^* value also show that Jenny 7 exhibited the smallest ΔE_{00}^* color difference value of 2.51 relative to the red proof (Table 5), and that the simulated color of Jenny 7 was also qualitatively consistent with that for the red proof (Table 5). Table 5 also shows Jenny 3 had the greatest ΔE_{00}^* difference value of 7.4 relative to the red proof, and this difference is largely a function of the low L* values measured for Jenny 3.

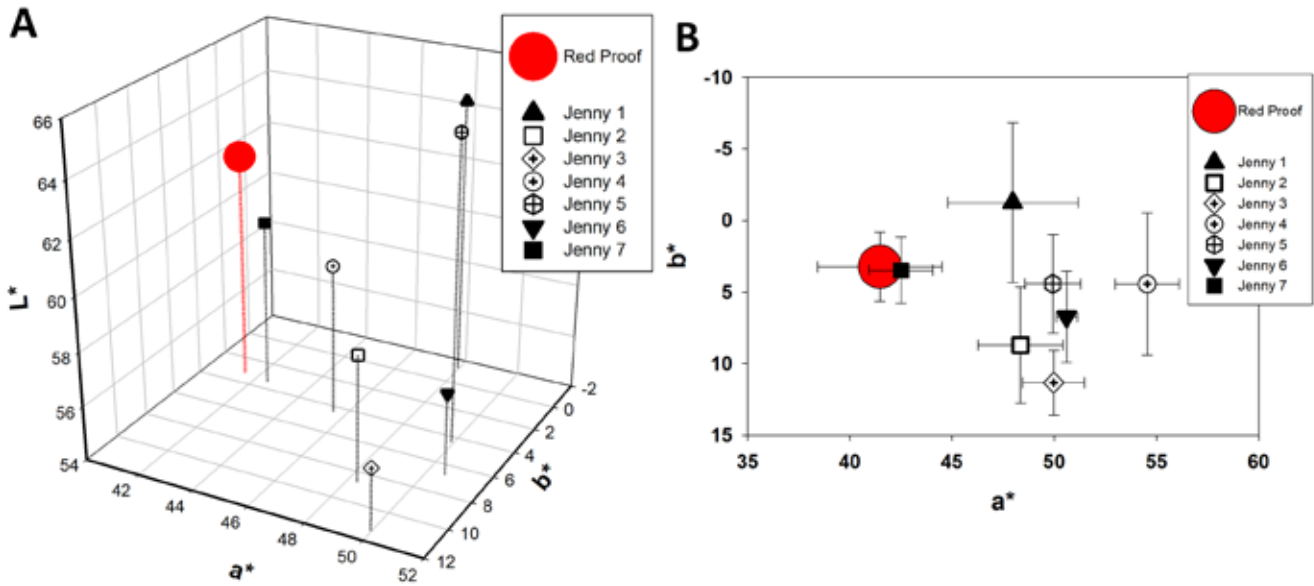


Figure 5. A) 3D plot of average values of L*, a*, and b* for the red data B) Plot of the mean values a* and b* with the a* and b* population standard deviations for the red data.

Standard Error of Mean					
Group Name	N (Sample Size)	Sample Mean	σ	$\sigma/(N^{0.5})$	
Red Proof	50	41.47	3.05	0.431	
Jenny 1	6	47.97	3.19	1.302	
Jenny 2	6	48.35	2.09	0.853	
Jenny 3	6	49.97	1.51	0.616	
Jenny 4	6	54.55	1.56	0.637	
Jenny 5	6	49.93	1.36	0.555	
Jenny 6	6	50.6	0.51	0.208	
Jenny 7	6	42.5	1.56	0.637	

Source of Variation	Degrees of Freedom (DF)	Sum of Squares (SS)	Mean Square (MS)	F	P
Between Groups	7	1810.098	258.585	37.787	<0.001
Residual	84	574.828	6.843		
Total	91	2384.927			

Holm-Sidak:				
Comparison	Diff of Means	t	P	P<0.050
Red Proof vs Jenny 4	13.08	11.573	<0.001	Yes
Red Proof vs Jenny 6	9.13	8.078	<0.001	Yes
Red Proof vs Jenny 3	8.5	7.521	<0.001	Yes
Red Proof vs Jenny 5	8.46	7.485	<0.001	Yes
Red Proof vs Jenny 2	6.88	6.087	<0.001	Yes
Red Proof vs Jenny 1	6.5	5.751	<0.001	Yes
Red Proof vs Jenny 7	1.03	0.911	0.365	No

Table 4. ANOVA analysis for the red colors and Holm-Sidak comparison.









	L*	a*	b*	ΔE_{00}^*	Simulated Color
Red Proof	62.45	41.47	3.23	NA	
σ	2.79	3.05	2.42	NA	
Jenny 1	64.32	47.97	-1.25	5.49	
σ	4.78	3.19	5.58	2.12	
Jenny 2	58.68	48.35	8.70	5.39	
σ	2.57	2.09	4.06	2.00	
Jenny 3	56.27	49.97	11.33	7.40	
σ	0.74	1.51	2.28	1.02	
Jenny 4	59.62	54.55	4.45	5.61	
σ	2.31	1.56	4.98	0.61	
Jenny 5	65.15	49.93	4.43	4.19	
σ	1.94	1.36	3.44	0.58	
Jenny 6	57.05	50.60	6.73	6.03	
σ	2.07	0.51	3.19	1.92	
Jenny 7	60.25	42.50	3.48	2.51	
σ	1.85	1.56	2.31	1.24	

Table 5. Averages and standard deviations of L*, a*, b*, and ΔE_{00}^* of the red data for the proof and the 7 stamps with their simulated colors.

Color Validation

Given the two instruments' different optical setups, spectrometers, and detectors, the color differences obtained from the instruments were not

unexpected. Importantly, studies using multiple systems should seek to document differences relative to a standard if the comparisons of the data sets are made. Table 6 shows such a comparison between the VSC and MFT measurements relative to color







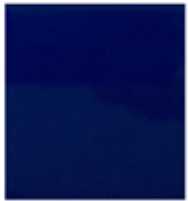


	Method	L*	a*	b*	ΔE_{00}^*	Simulated Colors	Actual Colors
Red Tile	Reference	32.00	61.20	48.40	NA	NA	
	VSC avg (n=6)	34.53	64.13	48.87	2.36		
	VSC σ	0.49	1.03	1.92	0.37		
	MFT Avg (n=3)	30.68	66.99	52.89	2.93		
MFT σ	2.53	2.05	4.37	0.86			
Green Tile	Reference	27.00	-18.10	7.30	NA	NA	
	VSC avg (n=6)	26.75	-19.17	6.75	1.17		
	VSC σ	0.69	1.15	0.70	0.47		
	MFT Avg (n=3)	21.97	-25.63	7.88	5.77		
MFT σ	2.28	0.75	1.90	1.07			
Blue tile	Reference	17.60	19.00	-39.20	NA	NA	
	VSC avg (n=6)	15.25	19.88	-38.95	1.81		
	VSC σ	0.38	1.11	0.68	0.12		
	MFT Avg (n=3)	10.56	25.71	-51.22	6.11		
MFT σ	1.10	0.98	0.80	0.57			

Table 6. Mean and the population standard deviation results comparing the VSC and the MFT color measurements of the red, green and blue reference tiles, with the simulated colors and images of the actual RGB color representation of the tiles for comparison.

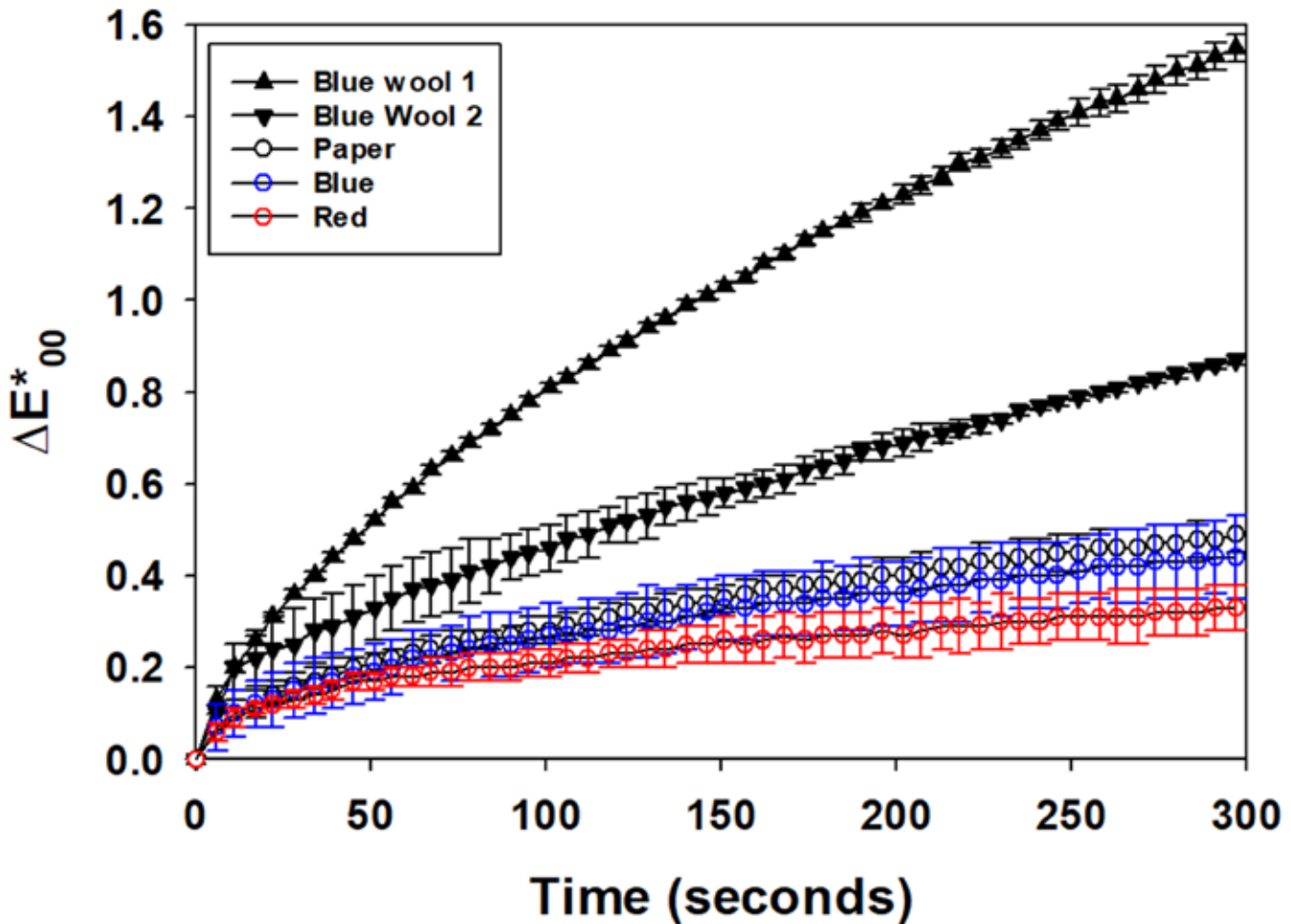


Figure 6. Plot of color difference measured by ΔE^*_{00} for the uncolored paper regions, six blue regions, six red regions for Jenny 7 in relation to blue wool 1 and blue wool 2.

tile references. The average difference for VSC spot measurements had ΔE^*_{00} color difference values of < 2.36 for all reference tiles. While MFT data yielded comparable ΔE^*_{00} color difference values for the red reference tile, ΔE^*_{00} color difference values of slightly > 5 were obtained for the green and blue tiles. A possible reason for the slightly elevated ΔE^*_{00} color difference values could be related to the low L^* values for the green and blue tiles. Since the MFT measurement is generated from a reflected color signal from a focused white light spot, the absorption of darker colors results in a smaller reflected light signal/noise ratio sent to the spectrometer. Such absorption will also take place for the VSC measurement, but with a smaller relative loss of signal given the dispersion of source light over the entire light chamber compared to the focused MFT source. Therefore, the marginal increase in ΔE^*_{00} color difference of the MFT is likely systematic in nature, and due to inherent optical differences between the two color measurement systems.

Microfade Testing

All MFT runs of the regions of interest shown in Figure 1B for Jenny 7 were performed for 300 seconds, with the results plotted in reference to the ISO blue wools. The ΔE^*_{00} color difference values reported represent the color change after 300 seconds of illumination. For this experimental session, the ISO blue wool 1 had an average ΔE^*_{00} color difference of 1.55 ± 0.03 (n=3); the ISO blue wool 2 had a ΔE^*_{00} color difference of 0.87 ± 0.01 (n=3) as shown in Figure 6. From the MFT results, the uncolored stamp paper, blue, and red regions all change at a rate < both blue wool 1 and blue wool 2 (Figure 6). The six uncolored paper regions were the most sensitive to light exposure, relative to red and blue regions, and had an average ΔE^*_{00} color difference of 0.49 ± 0.04 . The red regions had an average ΔE^*_{00} color difference of 0.33 ± 0.05 (n=6), which is statistically different from the change noted in the white/uncolored regions of the paper. The blue regions had average ΔE^*_{00} color difference of 0.44 ± 0.09 (n=6), and the blue region

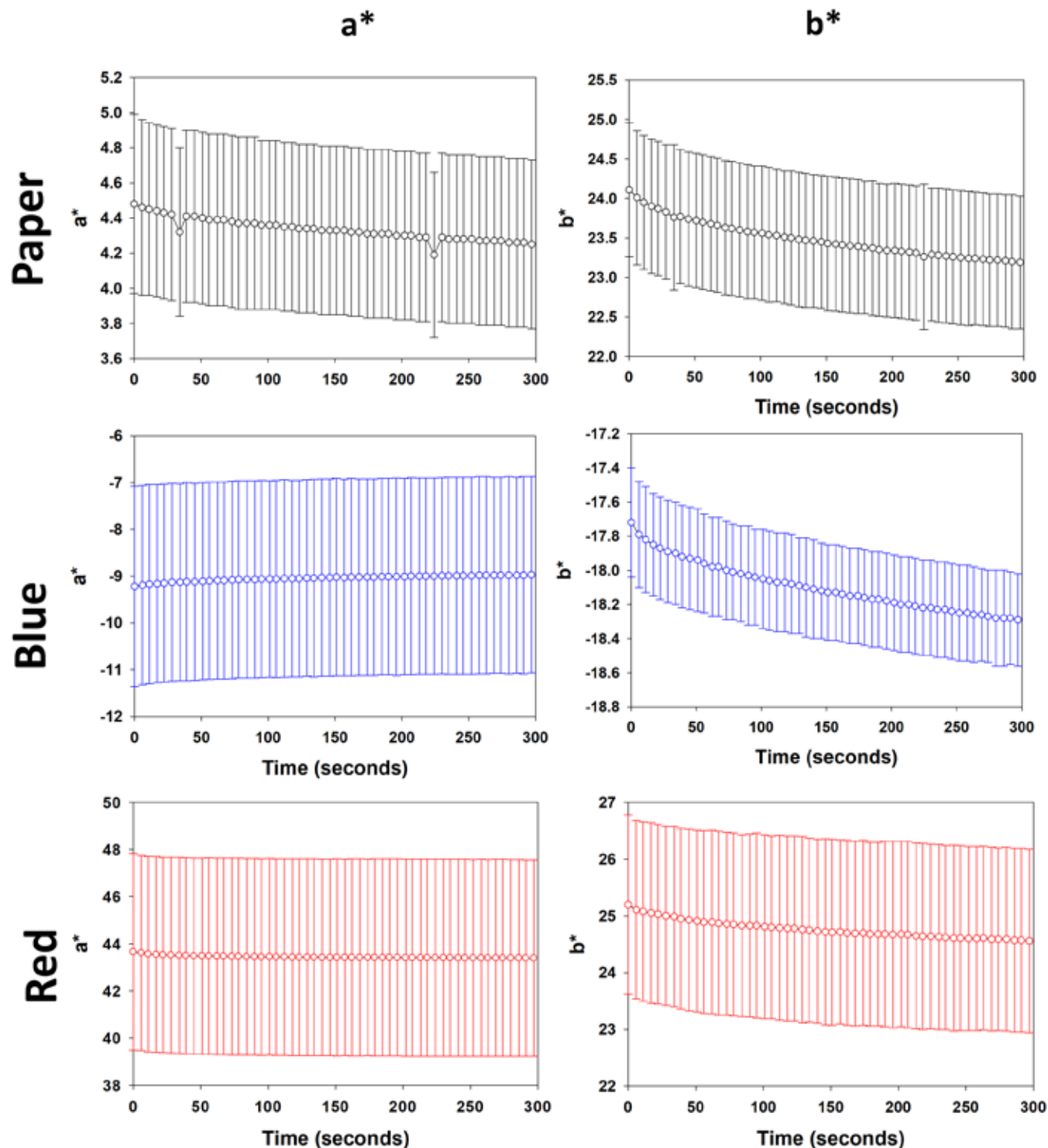


Figure 7. The plots of a^* and b^* changes for MFT as a function of time for the paper material, red, and the blue regions for Jenny 7.

fading behavior was intermediate between rate of change for white/uncolored paper and red regions. The stamp faded more slowly than blue wool 2, which suggests exhibition lighting could be designed to handle up to a maximum of 1.2 Mlux-h below the “Just Noticeable Difference/Fade” (JND/JNF) (Lowe, Smith et al. 2017) threshold for the life of the

object, which has been reported to be equivalent to a ΔE_{00}^* of ≈ 1.6 (Ford and Druzik 2013); it should be noted that JND/JNF is an approximation with other perception ranges reported and the topic of “acceptable” color change is considered endlessly debatable (Michalski and Dignard 1997). For reference, if the stamp paper and colors faded more rapidly than blue

wool 2, a more conservative exhibition light level of a maximum of 0.4 Mlux·h would have been advised for the life of the object (Lowe, Smith et al. 2017).

L^* values of all the test regions were found to be constant during the tests. For the stamp paper, a^* and b^* both decrease during the MFT (Figure 7) indicating a slight decrease in red and a shift from yellow to less yellow respectively. For the blue regions, very slight increases in a^* (green to less green) with a noticeable decrease in b^* (increasing blue). While for the red regions, a^* is constant while b^* decreases indicating a small shift from yellow to less yellow (Figure 7).

Discussion

Color difference by ΔE_{00}^* is a more robust representation of expressing color differences relative to color difference by ΔE_{ab}^* , because it corrects for the perceptual non-uniformities of CIELAB values of the CIELAB system (Luo, Cui et al. 2001), and has values roughly half the magnitude of an equivalent ΔE_{ab}^* value (Ford and Druzik 2013). In particular, the analysis of the blue colors showed Jenny 6 yielded the smallest color difference as it had the lowest ΔE_{00}^* value. However, based upon the mean values for a^* and b^* one would have identified Jenny 2, 3 and Jenny 7 as being most similar to the Jenny blue proof, not Jenny 6. The explanation for these seemingly disparate results stems from the fact that the differences in L^* values are only accounted for when color difference by ΔE_{00}^* is computed. Even when the ΔE_{00}^* calculation is performed, it should be noted that there is not a single-color value that represents any of the Jenny's regions - red, blue, or uncolored- even within an individual stamp. Instead, there exists a range of color values that are defined by statistical spread in measurements. Recognizing that L^* , a^* , and b^* coordinates for these stamps cluster about a value, rather than defining a unique set of values, is important to understand. Appreciating that there is a distribution of color values for an object, rather than a solitary color, is most important with respect to MFT results since the goal of the technique is to measure a shift in color where the starting color value is not uniquely fixed but is locally diffuse. Finally, we note that the non-linear nature of color fading in general may mean that the Jenny stamps experienced more rapid loss of color in the years following printing relative to the 100+ year old object examined in this study.

MFT is a useful tool for the curation of artifacts, but it is important to consider its limitations (Ford and Druzik 2013). MFT is designed to provide data for materials classified as light sensitive, meaning materials that would be able to handle 3.6 Mlux·hrs of lighting at a maximum. MFT cannot predict nonphotochemical changes, such as long term polymer degradation or biological attack (Ford and Druzik 2013). In MFT, the term 'reciprocity' is used to correlate accelerated laboratory color fading with that expected for objects experiencing lower illumination levels used during exhibition display, and an assumption is made that color shift depends only upon the total exposure dose. Such a reciprocal relationship can fail when chemical reactions occur owing to induced local heating or dehydration reactions (Ford and Druzik 2013). Even the MFT color measurement itself has been reported as a source of uncertainty (Ford and Druzik 2013), which is why the color comparisons presented here are regarded as a focal point of this study.

To evaluate differences between color measurements systems, a set of VSC data was collected using a dedicated white reference tile (used in the MFT portion of the study) for Jenny 7, the stamp whose colors most closely approximate the blue and red of the Jenny proofs. The ΔE_{00}^* color difference for the colors and paper have a difference value of 5.48 and have a consistent simulated color output as shown in Table 7, and are qualitatively similar, particularly for the uncolored paper and blue regions of the stamp. As described in the color validation section above, differences between two data sets derived from two different measurement setups are not unexpected. The blue values from MFT for the stamp in the case of Jenny 7 were better than the blue tile in Table 6, which is likely because of the higher L^* of the blue color in the stamp. Though paper substrate was used as the white reference in the VSC color measurements and yielded color information about the pigment free of the substrate; a white tile reference was used for comparison of the VSC and MFT data since the MFT measurement contains the color pigment on the substrate. This is needed to eliminate a potential systematic error in the difference calculations. The similarity in the L^* , a^* , and b^* values obtained for the two-color measurements systems, and their simulated output, allow for a reasonable level of confidence in comparing the experimental color changes with the color data for the Jenny stamps.

For the a^* and b^* data for both the blue and red regions of the Jenny stamp, the ANOVA results

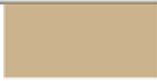





	L*	a*	b*	ΔE_{00}^*	Simulated
VSC Paper Color	74.03	2.47	22.30	NA	
VSC σ	0.68	0.68	2.35	NA	
MFT Paper Color	71.77	4.48	24.11	2.80	
MFT σ	1.49	0.51	0.85	0.78	
VSC Blue	34.87	-7.27	-15.08	NA	
VSC σ	1.53	1.79	1.45	NA	
MFT Blue	32.62	-9.22	-17.72	3.65	
MFT σ	2.25	2.14	0.32	1.40	
VSC Red	43.87	39.77	17.30	NA	
VSC σ	1.15	1.57	3.10	NA	
MFT Red	47.6	43.66	25.5	5.48	
MFT σ	1.81	4.17	1.58	1.46	

Table 7. Mean and population standard deviations for L*, a* and b* comparisons of VSC and MFT for the different colors of Jenny 7 with VSC data using a dedicated tile for a white reference as opposed to stamp paper.

showed Jenny 7 to be the most similar to the blue and red proofs. As a result of their statistical similarity, Jenny 7 and the blue and red proof color data have been grouped as a shaded area in Figure 8A and 8B respectively. From the additional light exposure from the MFT, blue regions experienced a slight increase in a* by 0.16 units, while b* decreased 0.57 units, while for the red regions a* was constant and b* decreased by 0.64 units. The vectors representing these changes are depicted in Figures 8A and 8B. Those vectors are represented as arrows initiated from the grouped shaded areas of the proofs plus Jenny 7, and proof plus Jenny 2, 3, and 7 for the red and blue regions respectively. Note that the vector is scaled by up a factor of 10 x to show the direction of the color change expected for the stamp when displayed under museum exhibition lighting conditions. Also note that the representation of the color shift arrow is not quantitative and is provided as a graphical aid. The history of the lighting conditions Jenny 1-7 have suffered is not known to us, but it is important to note that the MFT setup is designed with UV and IR cutoffs beyond which natural lighting will extend (Whitmore, Pan et al. 1999). Specifically, long term exposure to lighting with a UV component, namely sunlight, would yield results the MFT is not designed to explain. Fading from sunlight exposure is then a potential explanation for the reported a* values > 1 σ in comparison to the proofs. This is most clearly shown for the red region data (Figure 8B), whereas the blue regions showed a significant degree of overlap with the blue proof (Figure 8A).

The previously described NPM limits on exposure of paper-based objects to 54 Candela steradian/square meter (5 footcandles (fc) or 54 lux) for no more than three (≈ 0.04 Mlux·h) to six months (≈ 0.08 Mlux·h) at a time assuming eight to ten hours of exhibition per day falls within the maximum of 1.2 Mlux·h for the lifetime of the object. In fact, the current lighting plan designed for the National Postal Museum's *Gems of American Philately* exhibition, which opened in 2013, features a gradient plan in which visitors enter the William H. Gross Stamp Gallery at a light level of 54 Candela steradian/sq m (5 fc) and slowly transition to even lower light levels of 21.5 -32.3 Candela steradian/sq. m (2-3fc) in the *Gems of American Philately* exhibition. As an added measure to protect the philatelic objects exhibited in *Gems of American Philately*, the exhibit cases are equipped with motion sensors that activate only when a visitor steps directly in front of a recessed wall mounted exhibit case. Once activated, the fiber optic lights inside the exhibit case are engaged for only 20 seconds at a time. Daily monitoring is required to track visible damage and to ensure that all elements of the lighting plan are functioning as designed. Broken window shades, motion sensors, and lighting components must be identified and repaired immediately to ensure that light levels do not exceed established limits. Working closely with building facilities staff and museum security to cover cases or temporarily remove objects from exhibition until problems can be resolved is an essential aspect of managing long term exhibition of light sensitive materials and a key factor in the successful implementation of any lighting plan.

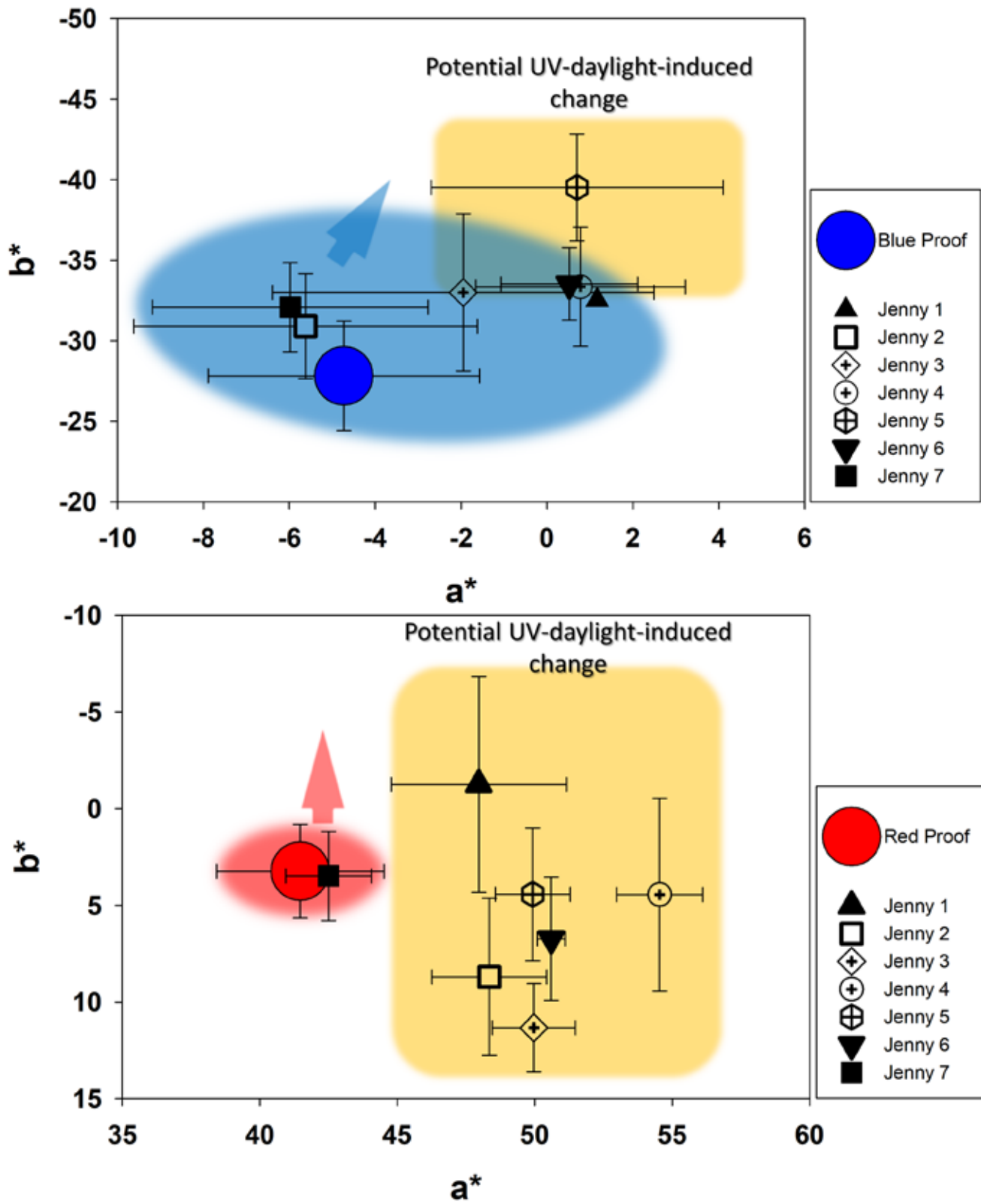


Figure 8. Direction of potential color shift on the a^* and b^* plot of the blue and red color data for the Jenny A) blue regions and B) red regions. Blue and red shaded areas represent the grouping of Jenny 2, 3, and 7 with the blue and Jenny 7 with the red proof data respectively. Blue and red arrows represent the vector of MFT color fading (see text) and the yellow shaded regions represent a color potentially owing to exposure to sunlight.

	≈ exposure for a day	10 yr Calculated Maximum Light Exposure
100 views/day	0.56 h	0.056 Mlux·h
250 views/day	1.4 h	0.14 Mlux·h
500 views/day	2.8 h	0.27 Mlux·h
1,000 views/day	5.5 h	0.55 Mlux·h

Table 8. Tabulated calculations of daily exposure duration and projected decadal light exposure based on viewing frequency which is well under the 1.2 Mlux·h limit.

This careful approach to exhibition management and lighting plan design has improved the visitor experience by making some of the most precious objects in the national collections permanently available for viewing without overexposing the objects to unnecessary light. Such an approach is consistent with the calculations presented in Table 8. Even using an assumption of 1000 views/day lighting at 26.9 Candela steradian/square meter for 10 years, this would result in a maximum lighting exposure of 0.55 Mlux·h, which is well below the 1.2 Mlux·h limit. Because 1000 views/day is likely on the high end of visitor frequency, data for 100 views/day, 250/day and 500/day were also tabulated. These new data and calculations affirm that the conservative approach being taken at the National Postal Museum has been successful in protecting collection material during the nearly ten years that the *Gems of American Philately* exhibition has been open. Daily gallery checks and periodic condition surveys of the objects on view have additionally revealed no visible changes in color or appearance.

Conclusions

High accuracy color measurements for the bi-colored 1918 Curtiss Jenny airmail stamp were achieved and verified using color fast reference materials. These measurements were consistent with a second independent system used to measure color changes following accelerated light exposure under laboratory conditions, according to a rigorous method to compare color space coordinates. Additionally, digital simulations of these color values allow one to qualitatively assess such comparisons.

Museum exhibition lighting conditions for the inverted Jenny should not exceed 1.2 Mlux·h over the lifetime of its public exhibition to ensure that color changes remain below the just noticeable threshold of $1.6 \Delta E_{00}^*$ color difference units. Experimental light exposure of the Jenny indicated the blue portions of the stamp underwent a color change broadly consistent with the small differences observed between

the 1918 blue vignette proof and the color values for the stamps examined. However, color fade testing offered no insight into differences observed for the color change between the red frame in the red proof relative to the red color measured in the examined stamps. The significant difference between the two disparate color change vectors for the red regions of the Jenny suggests that UV-daylight exposure may be responsible for color differences observed between the proof and the vast majority of the stamps. There exist many opportunities to extend such laboratory color analysis to other stamps of interest to the philatelic community, and we hope this study provides a methodological framework for those future efforts to predict color changes in exhibition settings. In future efforts, we plan to turn our attention to characterizing the compositional nature of the blue and red inks used to print the Jenny to gain a material-based understanding for the color differences observed.

Acknowledgements

Allyce McWhorter from Foster and Freeman is thanked for introductory color measurement training and general VSC8000HS instrumentation resource. We are grateful to Dan Piazza from the National Postal Museum for interesting discussions on the topic of 1918 Curtiss Jenny US airmail stamp. We also thank Beth Heydt and Kelly Cooper from NPM who assisted in making the vignette for 24¢ stamp; plate number 8493 (National Postal Museum, object number 0.242263.15824 and 24¢ stamp carmine frame: for USA Scott C3; plate number 8492 (National Postal Museum, object number 0.242263.15825) available for color analysis.

References

- Allen, J. A. and T. Lera 2012. *The U.S. 1851 3¢ Stamp Color, Chemistry, and Changes*, The Institute for Analytical Philately
- Caswell, L. R. 2012. *Reflectance Spectroscopy of Colored Overprints*, The Institute for Analytical Philately.

- Charles, H. K. 2017. *Exploring Color Mysteries in the United States Large and Small Numeral Postage Due Stamps using X-ray Fluorescence Spectrometry*, The Institute for Analytical Philately.
- Charles, H. K. 2020. *1894 and 1895 Series First Bureau Postage Due Stamps: Questions of Color, Fluorescence, and Early Use: Part I. IV*, The Institute for Analytical Philately.
- Cibulski, J. M. 2015. *Resolving the Scanner Dependency in Color Matching*, The Institute for Analytical Philately
- Cibulski, J. M. 2015. *Towards a Stamp-Oriented Color Guide: Objectifying Classification by Color*, The Institute for Analytical Philately.
- Cibulski, J. M. 2017. *The Colors of the German Crown and Eagle Series: A Tutorial on the Objective Determination of Color Varieties*, London, UK, The Institute for Analytical Philately.
- DeBlois, D. and R. D. Harris (2011). The Colors of Martin Van Buren: An Engraved Postage Stamp (1938-1959). *The Prexie Era-The Newsletter of the USSS 1938 Presidential Era_Study Group* 52.
- EasyRGB. Retrieved 10/14/2022, 2022, from <https://www.easyrgb.com/en/convert.php#inputFORM>.
- Engraving Division, Bureau of Engraving and Printing. 1960. "Stamp History 24¢ Air Mail Stamps (Airplane)."
- Ford, B. and J. Druzik 2013. "Microfading: the state of the art for natural history collections." *Collections Forum* 27(1-2): 54-71.
- Invoice from Gebr. Heyl & Co. Manufacturers of chemical colors to Government of the United States of North-America, Bureau of Engraving and Printing. 15 January. RG 0318 (Bureau of Engraving and Printing) A1 12 (Central Correspondence Files 1881 - 1949). Container 35 (1917. Travel THRU 1917: ACCTS: Govt. Prop. Sold) Folder titled "ACCTS: COLORS" U. S. National Archives and Records Administration (NARA).
- Hisey, R. 2020. *Single Pixel Colorimetry and Optical Densitometry in Philately.*, The Institute for Analytical Philately.
- Hofmeyr, J. 2020. *A Quantitative Color Analysis of the US 3¢ 1861 Issue*, Virtual, The Institute for Analytical Philately.
- Letter from Director James Wilmeth to Mr. Wilfred A. French. 30 July 1918. RG 0318 (Bureau of Engraving and Printing) A1 12 (Central Correspondence Files 1881 - 1949). Container 44 (1918: Paper: Internal Revenue THRU 1918: Publications). Folder titled "Postage Stamps: Colors 1918" U. S. National Archives and Records Administration (NARA).
- Judge, R. H. 2015. *The Admiral Issue of Canada: A Colorimetric and XRF Study of the Carmine 2¢ Issue*, The Institute for Analytical Philately.
- Kirker, J. (2006). "24c Curtiss Jenny single." Retrieved 15 October 2022, from [HTTPS://POSTALMUSEUM.SI.EDU/OBJECT/NP-M_1980.2493.10009#COPY_LINK](https://postalmuseum.si.edu/object/NP-M_1980.2493.10009#COPY_LINK).
- Kuzio, O. (2018). Excel Sheet to Calculate DE2000 from CIE L*, a*, b*
- Laudato Beltran, V., et al. (2021). Microfade Tester: Light Sensitivity Assessment and Role in Lighting Policy. Los Angeles, CA, J. Paul Getty Trust.
- Lera, T., et al. 2012. *A Scientific Analysis of the First Issues of Chile 1853-1862, London Printing*, The Institute for Analytical Philately.
- Lowe, B. J., et al. 2017. "Light-ageing characteristics of Māori textiles: Colour, strength and molecular change." *Journal of Cultural Heritage* 24: 60-68.
- Luo, M. R., et al. 2001. "The Development of the CIE 2000 Colour-Difference Formula: CIEDE2000." *Color Research and Application* 26(5): 340-350.
- Materials Technology,. (12/22/22). "The Blue Wool Scale." 2022, from [HTTP://WWW.UVWEATHERING.COM/UV_SCALE.HTML](http://www.uvweathering.com/uv_scale.html).
- Mckee, A. 2015. *Paper and Color Varieties of the People's Republic of China "Workers and Soldiers" Definitive Set of 1955-1961*, The Institute for Analytical Philately
- Michalski, S. and C. Dignard 1997. "Ultrasonic misting. Part 1, experiments on appearance change and improvement in bonding." *Journal of American Institute for Conservation* 36(2): 109-126.
- Letter from N. Underwood in Ink Making Division to Director James Wilmeth. 24 July 1918. RG 0318 (Bureau of Engraving and Printing) A1 12 (Central Correspondence Files 1881 - 1949). Container 44 (1918: Paper: Internal Revenue THRU 1918: Publications). Folder titled "Postage Stamps: Colors 1918" U. S. National Archives and Records Administration (NARA).
- Robert A. Siegel Auction Galleries, I. (2017). The Don David Price Award-Winning Collection of the 1918 24-cent Jenny Air Post Issue Featuring the Inverted Jenny Position 28 and the Original Robey Sale Letter. New York, Robert A. Siegel

- Auction Galleries, Inc.
- Robertson, A. R. 1977. "The CIE 1976 Color-Difference Formulae." *Color Research and Applications* 2(1): 7-11.
- Świt, P., et al. 2021. "Beam characterization of a microfading tester: evaluation of several methods." *Heritage Science* 9.
- Thomson, G. 1978. *The Museum Environment*. London, Butterworth-Heinemann.
- Letter from Treasury Department to Speaker of the House of Representatives. 26 June 1917. RG 0318 (Bureau of Engraving and Printing)) A1 12 (Central Correspondence Files 1881 - 1949).
- Container 35 (1917. Travel THRU 1917: ACCTS: Govt. Prop. Sold) Folder titled "ACCTS: COLORS" U. S. National Archives and Records Administration (NARA).
- USPS (2022). "Rates for Domestic Letter Since 1863." Retrieved 12/20/22, 2022, from [HTTPS://ABOUT.USPS.COM/WHO/PROFILE/HISTORY/PDF/DOMESTIC-LETTER-RATES-SINCE-1863.PDF](https://about.usps.com/who/profile/history/pdf/domestic-letter-rates-since-1863.pdf).
- Whitmore, P. M., et al. 1999. "Predicting the Fading of Objects: Identification of Fugitive Colorants Through Direct Nondestructive Lightfastness Measurements." *Journal of American Institute of Conservators*: 395-409.

Glossary list of terms:(in order of appearance in the text)

Candela steradian/square meter – is the SI (International System of Units) unit of illuminance and luminous emittance in a specific direction and takes into account the angular distribution of the light.

Footcandles – a non-SI unit defined as illuminance on a one square foot surface from a uniform source of light.

Lux – the SI unit of measure for illuminance, i.e. the amount of light falling on a surface per unit area.

Region of interest – an area selected for analysis

Microfade testing (MFT) – MFT is a non-contact and "virtually non-destructive" method for determining small increments of reflectance color shift on cultural heritage materials (Ford and Druzik 2013). The technique uses a light source (originally xenon, but now LED systems have been developed), to generate a spectral distribution of visible wavelengths ≈ 370 nm to ≈ 760 nm (Whitmore, Pan et al. 1999); which for this design was filtered through components comprising a "Fading Test System" (Newport Oriel Corporation), where the light is focused onto an object by fiber optics.

Dark reference – the background current in a charge coupled device (CCD) measured periodically by use of a shutter, and this background is then subtracted from spectral measurements.

White reference – spectrum for a material that has little to no features across the range of wavelengths measured. For this study a 99% calibrated Spectralon® diffuse reflectance standard from Labsphere, Inc., (a proprietary polytetrafluoroethylene (PTFE) materi-

al) was used.

Full width at half the maximum (FWHM) – a figure of merit for spectral resolution, in this case a one dimensional spatial measure of intensity across a focused spot of white light. From such a plot the width at half the maximum intensity is defined as the full width at half max.

ISO Blue wool standards – International Organization for Standardization (ISO) blue wool standards are a series of eight blue dyed woven textiles ranging from blue wool 1 to blue wool 8 that have documented light sensitivities originally developed for the textile industry. The lower number blue wools are the most light sensitive and increasing blue wool numbers require increasing light dosage to fade (Technology). In making MFT measurements from blue wools, the topography (height variation) of the woven wools has to be taken into consideration. Measurements must be taken on the top surface of a weave and not from a valley. With the neutral density filter in place, the positioning to the top of weave will result in the brightest spot and can be confirmed through the endoscope magnifier.

CIE-L*a*b Color space coordinates (L*,a*,b*) – stands for the International Commission on Illumination (CIELAB) color space coordinates L*, a*, b*. CIELAB color space coordinates of L* is expressed on the z-axis and represents the lightness to darkness value, the a* is for red/green axis, and b* for the yellow/blue axis (shown in Figure 3A).

DE_{ab} , DE_{76} – Color difference in terms of ΔE_{ab}^* is calculated using the following equation (CIE 1976):

$$\Delta E_{ab}^* = \sqrt{(L_0^* - L_t^*)^2 + (a_0^* - a_t^*)^2 + (b_0^* - b_t^*)^2} \quad (\text{eq.1})$$

For eq.1, L_0^* , a_0^* , b_0^* are L^* , a^* , and b^* collected at time zero, while L_t^* , a_t^* , b_t^* are values after time t has elapsed.

DE_{2000} – The color difference by DE2000 or ΔE_{00}^* formula is (Luo, Cui et al. 2001):

$$\sqrt{\left(\frac{\Delta L'}{k_L S_L}\right)^2 + \left(\frac{\Delta C'}{k_C S_C}\right)^2 + \left(\frac{\Delta H'}{k_H S_H}\right)^2 + R_T \frac{\Delta C'}{k_C S_C} \frac{\Delta H'}{k_H S_H}} \quad (\text{eq. 2})$$

The color difference by ΔE_{00}^* takes into account the perceptual non-uniformities of the CIELAB color space by implementing mathematical five corrections to aspects of color attributes within the formula: 1) correction for neutral colors using $\Delta L'$, $\Delta C'$, and $\Delta H'$ terms; 2) a lightness to darkness correction term,

$\left(\frac{\Delta L'}{k_L S_L}\right)^2$; 3) a chroma correction term, $\left(\frac{\Delta C'}{k_C S_C}\right)^2$

4) a hue correction term, $\left(\frac{\Delta H'}{k_H S_H}\right)^2$; and 5) the R_T function, which is an interactive term between chroma and

hue differences, $R_T \frac{\Delta C'}{k_C S_C} \frac{\Delta H'}{k_H S_H}$. Note that chroma, which is defined as purity of a color; hue, which refers to the color family, namely, a position on a color wheel; (Laudato Beltran, Pesme et al. 2021),

and the R_T function are all specifically designed to improve the color difference equation for chromatic differences in the blue region (Luo, Cui et al. 2001). The five correction terms implemented within the ΔE_{00}^* formula include the L^* , a^* , and b^* inputs and requires a rigorous description of color; further details regarding this color space are described by Luo and co-authors (Luo, Cui et al. 2001) and are outside the scope of this paper.

Light fastness – chemical stability of a color to long exposure of light.

Standard deviation (σ) of the population - the statistical spread of an average value of randomly distributed data. Since the deviation can be positive or negative, the spread of the data that results in plus or minus one or two standard deviations lies within the bounds of random chance to within 68 % (1 σ) or 95 % (2 σ) percent confidence respectively.

Analysis of variance (ANOVA) – compares data population variances /standard deviation (σ) of the group of interests to a control group.

Holm-Sidak method/P value – method to statistically compare observations with a cutoff for dissimilarity at > 95% chance.

Mlux·h – is mega lux hours, which is equivalent to 1,000,000 lux hours (lux·h).